Proceedings of CONF-CDS 2026 Symposium: Machine Learning and Neural Network Applications in Engineering
DOI: 10.54254/2755-2721/2026.AST37057

Assistive Input Device for Users with Limb Impairments

Xuanting Chen

Shenzhen College of International Education, Shenzhen, China
54374048@qq.com

Abstract. Individuals with severe limb impairments encounter substantial barriers during human-computer interaction, while commercially available assistive input devices are often prohibitively expensive. This paper presents a low-cost wearable assistive input device (bill-of-materials cost < ¥130) built around the nRF52832 Bluetooth-Low-Energy (BLE) system-on-chip and an MPU-6050 inertial measurement unit. A real-time-clock-based asynchronous event-driven architecture reduces power consumption, and the sensor's on-chip 5 Hz digital low-pass filter suppresses involuntary muscle tremor at the signal source. A multi-threaded PC-side client maps real-time posture data to discrete keyboard commands. A user study with three participants exhibiting distinct physiological profiles was carried out under two interaction modes. In discrete click-trigger mode, the system achieved a peak directional-selection throughput of 12 WPM, while continuous dwell-hold control yielded an average throughput of 4.2 WPM. The participant with a full, unrestricted range-of-motion (ROM) reached a trigger accuracy of 98.2 %, whereas the participant with severely-restricted head movement obtained only 64.0 % accuracy. Experimental results demonstrate that fixed-cutoff on-chip filtering carries inherent performance limitations for users with extremely limited motion range. Directions for future work include adaptive filtering algorithms and multi-modal interaction schemes.

Keywords: assistive technology, wearable input device, human-computer interaction, inertial measurement unit (IMU), Bluetooth Low Energy (BLE), head-motion tracking, tremor suppression

1. Introduction

While modern information technology benefits the general public, people with severe limb impairments encounter prominent HCI barriers. This study is motivated by a real case: a bilateral upper-limb amputee could not operate standard input devices for e-commerce work, and speech recognition failed due to regional accents. This creates an urgent demand for a low-cost, accent-independent hands-free input system based on subtle voluntary head or stump movements.Commercial assistive devices suffer from exorbitant pricing. High-end eye-trackers are unaffordable for most disabled users in China, making accessible HCI hardware a critical social equity issue as well as an engineering challenge.This project defines three design goals: low hardware cost, low-latency micro-motion detection for keyboard command mapping, and durable, low-power wearable performance.The main contributions are as follows: (1) a cost-effective

© 2026 The Authors. This is an open access article distributed under the terms of the Creative Commons Attribution License 4.0 (https://creativecommons.org/licenses/by/4.0/).

DOI: 10.54254/2755-2721/2026.AST37057

wearable prototype (nRF52832 + MPU-6050, BOM < ¥130) with RTC-based asynchronous low-power firmware; (2) on-chip filtering for tremor suppression; (3) a multi-threaded PC client for low-latency posture-to-keystroke conversion; (4) systematic user evaluation with three physiologically distinct participants to test accuracy, latency and throughput.The system is optimized for full-day operation, sub-second interaction latency, and anti-drift capability, guiding the design of the filtering algorithm, power management scheme and decoding architecture.

2. Literature review

Hands-free computer-input technologies can be grouped into four major categories.First, vision-based eye-tracking and head-tracking solutions such as Camera Mouse [1] and electro-oculography (EOG) systems [2] achieve high pointing accuracy and require no physical contact. However, their performance is sensitive to camera placement, ambient-lighting variations and repeated system calibration. In addition, eye-gaze selection still suffers from the well-known "Midas-touch" problem of unintended activation.Second, inertial-sensor-based head-motion interfaces [3] are low-cost and lighting-independent, and can provide a viable alternative communication pathway for individuals with cerebral palsy and disordered head movements. The gradient-descent orientation filter developed by Madgwick et al. [4] has become a widely-adopted standard algorithm for accelerometer-gyroscope sensor fusion.Third, electromyography (EMG)-based interfaces [5] directly capture muscle-activity signals and are well-suited for users with upper-limb impairments, although electrode slippage and signal drift remain persistent practical limitations.Fourth, tremor-reduction techniques relying on biomechanical loading or notch-filtering have been validated on robotic rehabilitation orthoses [6]. Those studies confirm that involuntary high-frequency oscillatory motion can be algorithmically separated from voluntary user-initiated movement.

Despite substantial progress in this research field, two noticeable research gaps persist. Most published systems optimize either signal quality or hardware affordability, but rarely address both objectives simultaneously. Furthermore, very few existing assistive-device studies conduct formal user testing on participants with severely-restricted head-motion range — exactly the demographic that would most benefit from head-controlled interfaces. This paper therefore presents a low-cost IMU-BLE wearable prototype equipped with on-source tremor-suppression filtering, and reports user-test results collected from three participants with different physiological profiles, including one participant with severely-limited head-motion ROM.

3. Methodology

3.1. System architecture

The hardware system follows a perception-processing-transmission pipeline consisting of three tightly-coupled functional modules. A power-management circuit built around the HT73XX low-dropout-regulator chip converts battery voltage to a stable 3.3 V supply rail and suppresses high-frequency power-supply ripple noise that would otherwise degrade inertial-sensor readings. The MPU-6050 six-axis inertial-measurement unit forms the perception layer, sampling tri-axial acceleration and angular-velocity data transmitted to the microcontroller over the I2C (TWI) serial bus. The nRF52832 system-on-chip performs posture-computation tasks and transmits processed directional commands to the host PC via BLE notification packets. The MPU-6050 sensor communicates over I2C using its default device address 0x68 (SCL/SDA). Gyroscope and

DOI: 10.54254/2755-2721/2026.AST37057

accelerometer full-scale measurement ranges are configured to ±250 °/s and ±2 g respectively, maximizing measurement sensitivity for subtle head- and stump-motion detection.

3.2. Posture estimation

Orientation angles are estimated by fusing data from two complementary sensors. The accelerometer provides drift-free tilt-angle reference measurements contaminated by high-frequency noise, while the gyroscope delivers high-quality angular-rate readings over short-time windows but accumulates integration drift over longer durations. Sensor data is combined via a complementary filter. The roll tilt angle derived from accelerometer measurements is defined in Equation (1). Gyroscope-derived orientation is obtained through discrete angular integration, shown in Equation (2). The two angle estimates are blended using weighting coefficient α, which assigns higher priority to gyroscope readings during fast high-frequency movements, and gradually increases accelerometer weight for low-frequency motion, as written in Equation (3).

$$\theta_{\text{acc}} = \arctan 2(a_y, \sqrt{a_x^2 + a_z^2}) \tag{1}$$

$$\theta_{\text{gyro},k} = \theta_{k-1} + \omega_k \cdot \Delta t \tag{2}$$

$$\theta_k = \alpha \cdot (\theta_{k-1} + \omega_k \cdot \Delta t) + (1 - \alpha) \cdot \theta_{\text{acc},k} \tag{3}$$

This complementary-filter implementation maintains long-term drift-free orientation estimates while preserving responsiveness to rapid intentional head movements. Compared to a full Kalman filter, it avoids heavy matrix-operation overhead, making it suitable for resource-constrained microcontroller hardware. In this implementation $\alpha = 0.98$, which assigns 98 % weighting to gyroscope samples at each 50-ms update step, while the remaining 2 % weight from accelerometer data slowly corrects accumulated gyro drift. This parameter combination is well-matched to the slow, deliberate head-control motions typical for assistive-device users.

3.3. Tremor-suppression filtering

Amputees and people living with motor-impairment conditions often exhibit involuntary high-frequency muscle tremor, which appears as high-amplitude noise superimposed on raw gyroscope angular-velocity signals. To avoid increasing CPU workload with software-implemented filtering, the on-chip digital low-pass filter (DLPF) of the MPU-6050 sensor is activated at the signal source. Filter configuration value 0x06 is written to register DLPF_CFG (register address 0x1A). This enables a first-order low-pass filter with −3 dB cutoff frequency set near 5 Hz, whose mathematical form is given in Equation (4). The 5-Hz cutoff removes tremor-related signal components above this threshold while preserving low-frequency voluntary-movement trajectories, improving the signal-to-noise ratio for all downstream processing stages.

$$H(s) = \frac{\omega_c}{s + \omega_c}, \quad \omega_c = 2\pi f_c \tag{4}$$

3.4. Power management

Long-term wearable operation rules out inefficient busy-wait polling firmware patterns. The firmware implements an RTC-triggered asynchronous event-driven power-saving scheme: the

DOI: 10.54254/2755-2721/2026.AST37057

system-on-chip defaults to System-ON deep-sleep mode. A software timer generates a hardware interrupt once every 50 ms (configurable). The processor wakes briefly to perform one I2C sensor read operation and send one BLE notification packet, before calling nrf_pwr_mgmt_run() to immediately re-enter deep-sleep mode. Under this duty-cycled operating pattern, average power consumption depends on the active-time duty-cycle fraction D, as expressed in Equation (5) [7]. BLE transmit power is reduced to −20 dBm for short-range desktop communication scenarios. Sensor data is transmitted via the Nordic UART Service (NUS) using a 128-bit UUID, leveraging the BLE Notify property for low-latency data passthrough. During firmware debugging, J-Link Real-Time-Transfer (RTT) logging writes debug text into a RAM-based ring buffer, generating microsecond-precision debug output without disrupting Bluetooth communication timing.

$$P_{\text{avg}} = D \cdot P_{\text{active}} + (1 - D) \cdot P_{\text{sleep}} \tag{5}$$

3.5. PC-side client program

Initial single-threaded client tests demonstrated that BLE data reception, control-logic computation and graphical-interface rendering tasks blocked one-another, introducing input latency and wireless-packet loss. The client was subsequently restructured as a three-threaded asynchronous framework:1. A bleak-based reception thread, responsible for receiving and parsing incoming BLE Notify sensor packets;2. A 125-Hz control-logic thread converting posture angles into operating-system-level directional keystrokes (W/A/S/D) using the pydirectinput library;3. A 20-Hz graphical-user-interface thread, independently updating runtime system-status indicators.

Since multiple threads read-from and write-to shared variables storing gyroscope coordinates such as latest_gx, mutual-exclusion locks (Mutex) were implemented to eliminate race-condition bugs that would otherwise produce erratic, jumping cursor movement.

3.6. Keystroke-mapping and performance metrics

In discrete CLICK mode, a single directional keystroke is triggered once measured tilt exceeds a fixed angular threshold. In continuous HOLD mode, the directional keystroke remains active for the entire duration that the user maintains the tilted posture.Direction-selection throughput is quantified using words-per-minute (WPM). In this metric definition, N = total number of completed directional selections and T = test-session duration (minutes). Five completed directional selections are counted as one equivalent "word". The angular trigger threshold balances the trade-off between false-trigger probability and system responsiveness, and must be recalibrated individually for each participant based on their available head-motion ROM. This threshold-tuning challenge is analyzed in-depth within Section 5.

Definition: Cross-axis error rate

Cross-axis error rate = number of unintended secondary-direction keystrokes ÷ total number of triggered directional selections.

3.7. Mechanical durability improvements

Users with severe limb-motor impairment cannot precisely control the force and orientation applied when plugging-in charging cables. The original surface-mount-device (SMD) Type-C connector on prototype revision 3 sustained repeated shear-stress damage, tearing solder pads from the printed-circuit board. For hardware Revision 4, the charging-port module was redesigned using a

DOI: 10.54254/2755-2721/2026.AST37057

through-hole Type-C socket, with four metal pins soldered completely through the PCB substrate. This upgrade drastically improves tensile-load and torsion-stress resistance, with negligible additional material-cost. This hardware revision, developed based on feedback from potential end-users, satisfies the durability design requirement and illustrates the fault-tolerant design philosophy for accessibility hardware.

3.8. System calibration and personalized configuration

At power-on, the system records one second of stationary sensor readings as the user's neutral baseline posture. All subsequent tilt-angle measurements are calculated relative to this zero-offset reference, eliminating angular bias caused by misaligned headbands or stump straps. Since trigger-threshold values are strongly dependent on each user's maximum head-motion range, a short calibration workflow captures each participant's comfortable maximum safe tilt angle, and automatically scales the trigger threshold to a fixed fractional proportion of that maximum angle. This per-user personalization workflow allows identical firmware to adapt to participants with full-range neck movement, severely-restricted ROM, and tremor-affected full-range head-motion profiles evaluated in the user study.

4. Results

Three participants were recruited for human-subject testing:P1 – bilateral-forearm amputee, full unrestricted head-motion ROM, no head tremor;P2 – high-level spinal-cord injury, maximum head-tilt ROM < 30° in every direction;P3 – cerebral-palsy sequelae, severe involuntary head tremor, full-range head-motion ROM.

Task A (Discrete-CLICK test): Each participant completed 40 randomly-presented directional-selection trials. Trigger accuracy, average reaction latency, and cross-axis error-rate were recorded. Task B (Continuous-HOLD maze-navigation test): Participants steered an on-screen block through a two-dimensional maze using sustained head tilt. Completion time and wall-collision counts were logged. Every participant repeated the maze navigation task three times, and median performance values were reported.

Table 1. Task-A (Discrete-CLICK-mode) experimental outcomes

Participant	Trigger Accuracy	Avg. Reaction Time	Cross-axis Error Rate
P1 (normal ROM, no tremor)	98.2 %	415 ms	1.1 %
P3 (normal ROM, severe tremor)	91.5 %	520 ms	4.6 %
P2 (severely-restricted ROM)	64.0 %	850 ms	28.5 %

Table 2. Task-B (HOLD-mode maze navigation) experimental outcomes

Participant	Completion Time	Collision Errors	Task Status
P1 (normal ROM, no tremor)	35.4 s	0	Completed
P2 (severely-restricted ROM)	—	14.6	Timed-out (120 s limit)

DOI: 10.54254/2755-2721/2026.AST37057

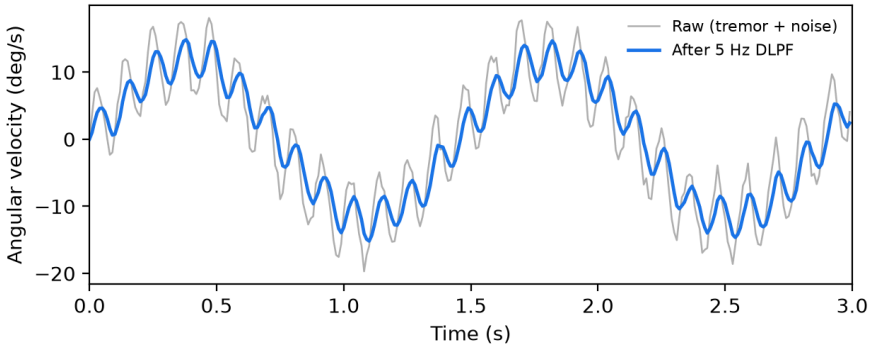

Figure 1. Angular-velocity waveforms: comparison of raw gyroscope signal (tremor + noise) and signal filtered via the 5-Hz MPU-6050 DLPF

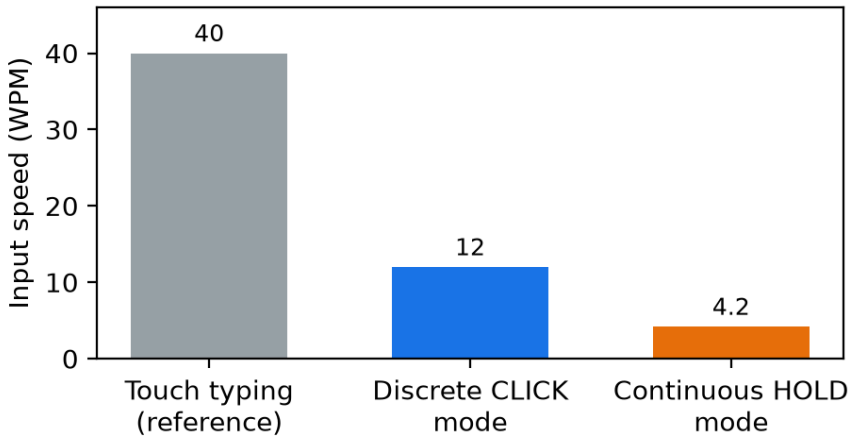

Figure 2. Direction-selection throughput comparison across interaction modes, with standard keyboard touch-typing speed shown as an external performance reference baseline

As shown in Figure 1, the on-chip DLPF effectively attenuates ~9 Hz tremor oscillations while retaining low-frequency voluntary head motion trajectories. Benefiting from this filtering, participant P3 with severe involuntary head tremor achieved a directional trigger accuracy of 91.5%, which is unattainable with conventional keyboards. Figure 2 presents the key throughput results: discrete click-trigger mode reached a peak input throughput of 12 WPM, close to its theoretical limit, whereas continuous dwell-hold mode only averaged 4.2 WPM, far lower than the conventional keyboard typing benchmark of 40 WPM.Obvious performance discrepancies existed among participants. P1 delivered fast and accurate inputs. In comparison, P2 required an extremely low angular trigger threshold to adapt to limited head motion ROM, resulting in a high cross-axis error rate of 28.5% and frequent delayed key releases. The sequential increase in average reaction latency (415 ms for P1, 520 ms for P3, 850 ms for P2) verifies that user physiological constraints, rather than BLE transmission or client processing overhead, dominate system response delay.The maze navigation Task B further validates continuous control performance. P1 completed the task in 35.4 seconds with zero collisions, while P2 timed out with an average of 14.6 wall collisions. This is mainly attributed to filter-induced signal lag that delayed key release during continuous head tilting. The performance gap between P1 and P2 reflects the combined negative impact of limited ROM and

DOI: 10.54254/2755-2721/2026.AST37057

filtering latency, independent of tremor noise. Meanwhile, P3's high task accuracy confirms the efficacy of the 5 Hz fixed-cutoff filter for tremor suppression.

5. Discussion

Experimental results reveal three key performance limitations of the proposed system. First, cross-axis motion coupling severely degrades accuracy for users with restricted head motion. To accommodate the limited range of motion of participant P2, a low angular trigger threshold was adopted. Since natural head movements are not strictly uniaxial, subtle lateral motions were falsely detected as valid inputs, yielding a high cross-axis error rate of 28.5%. This indicates that simple angle-threshold mapping lacks robustness for small-amplitude voluntary movements.

Second, the fixed 5 Hz on-chip low-pass filter introduces noticeable signal latency. Such temporal delay is further magnified by human visual feedback during fine head adjustments, which primarily caused P2's frequent collisions in maze navigation tasks.

Third, the 80 ms dwell-time requirement for continuous HOLD-mode typing imposes a theoretical throughput ceiling of 15 WPM. The low practical throughput of 4.2 WPM therefore stems from inherent interaction constraints rather than hardware or BLE communication limitations. While the fixed-cutoff filter effectively suppressed tremor noise and improved accuracy for tremor-affected user P3, a static filtering configuration fails to adapt to diverse user conditions, performing suboptimally for both fine limited motions and normal stable head movements.

This study also has methodological limitations. The small sample size (three participants) and single-session testing restrict statistical generalizability, and long-term user adaptation effects were not evaluated. Additionally, the signal analysis relies on representative waveforms instead of comprehensive raw datasets. Despite these constraints, the core findings remain valid. Crucially, the results prove that IMU sensing and BLE transmission are no longer the main bottlenecks. Future performance improvements should focus on adaptive interaction algorithms that better distinguish intentional gestures from involuntary motion.

6. Conclusion

This work presents an ultra-low-cost wearable head-motion assistive-input prototype with total bill-of-materials cost below ¥130. The system integrates an RTC-based asynchronous low-power firmware architecture, on-source tremor-suppression digital filtering and multi-threaded PC-side client software. Human-subject testing shows a peak directional-selection throughput of 12 WPM for discrete click-trigger mode, and an average throughput of 4.2 WPM for dwell-hold continuous control. Further performance analysis confirms that throughput bottlenecks stem from dwell-time requirements of the interaction scheme itself, not inertial sensing hardware or BLE wireless-transmission latency. Four concrete directions are proposed for future system improvement:1. Upgrade the fixed-cutoff filter to an adaptive-covariance Kalman filter, which adjusts smoothing strength dynamically based on measured angular-acceleration. This would enable heavy noise-smoothing for tiny corrective head-movements and near-zero-lag tracking for fast, large-amplitude voluntary motions.2. Add a supplementary trigger channel via low-cost EMG muscle sensors or mechanical bite-switches, decoupling directional posture-adjustment movement from click-trigger activation, and eliminating the 80-ms dwell-time requirement.3. Implement context-aware dynamic invisible-target boundary expansion, enlarging effective click-target zones based on contextual motion-history information, to reduce cognitive workload compared with traditional on-screen candidate-word prediction.4. Add nonlinear pointer-acceleration mapping:

DOI: 10.54254/2755-2721/2026.AST37057

small-amplitude head-tilt produces fine, slow cursor movement for precise control, while large head-tilt angles trigger rapid long-distance cursor travel, minimizing excessive neck rotation and physical fatigue for users with limited ROM.

References

[1] Betke, M., Gips, J., & Fleming, P. (2002). The camera mouse: Visual tracking of body features to provide computer access for people with severe disabilities. *IEEE Transactions on Neural Systems and Rehabilitation Engineering, 10*(1), 1-10. https://doi.org/10.1109/TNSRE.2002.1021581

[2] Barea, R., Boquete, L., Mazo, M., & Lopez, E. (2002). System for assisted mobility using eye movements based on electrooculography. *IEEE Transactions on Neural Systems and Rehabilitation Engineering, 10*(4), 209-218. https://doi.org/10.1109/TNSRE.2002.806829

[3] Raya, R., Rocon, E., Ceres, R., Harlaar, J., & Geytenbeek, J. (2011). Characterizing head motor disorders to create novel interfaces for people with cerebral palsy: Creating an alternative communication channel by head motion. *2011 IEEE International Conference on Rehabilitation Robotics*, 1-6. Zurich, Switzerland. https://doi.org/10.1109/ICORR.2011.5975409

[4] Madgwick, S. O. H., Harrison, A. J. L., & Vaidyanathan, R. (2011). Estimation of IMU and MARG orientation using a gradient descent algorithm. *2011 IEEE International Conference on Rehabilitation Robotics*, 1-7. Zurich, Switzerland. https://doi.org/10.1109/ICORR.2011.5975346

[5] Choi, C., & Kim, J. (2007). A real-time EMG-based assistive computer interface for the upper limb disabled. In *2007 IEEE 10th International Conference on Rehabilitation Robotics* (pp. 459-462). Noordwijk, Netherlands. https://doi.org/10.1109/ICORR.2007.4428465

[6] Rocon, E., Belda-Lois, J. M., Ruiz, A. F., Manto, M., Moreno, J. C., & Pons, J. L. (2007). Design and validation of a rehabilitation robotic exoskeleton for tremor assessment and suppression. *IEEE Transactions on Neural Systems and Rehabilitation Engineering, 15*(3), 367-378. https://doi.org/10.1109/TNSRE.2007.903917

[7] Siekkinen, M., Hiienkari, M., Nurminen, J. K., & Nieminen, J. (2012). How low energy is bluetooth low energy? Comparative measurements with ZigBee/802.15.4. In *2012 IEEE Wireless Communications and Networking Conference Workshops (WCNCW)* (pp. 232-237). Paris, France. https://doi.org/10.1109/WCNCW.2012.6215496